Layered material characterization using ultrasonic transmission. An inverse estimation methodology

María G. Messineo [a], Guillermo Rus [b], Guillermo E. Eliçabe [c], Gloria L. Frontini [a,c,*]

[a] Department of Mathematics, Engineering School, National University of Mar del Plata, Mar del Plata, Argentina
[b] Department of Structural Mechanics, University of Granada, Spain
[c] INTEMA-CONICET Material Science and Technology Research Institute, Mar del Plata, Argentina

ABSTRACT

This paper presents an inverse methodology with the aim to characterize a layered material through the identification of acoustical and mechanical properties of its layers. The framework to accomplish this objective is provided by the Inverse Problems (IPs) theory. Material characterization refers to the detection and localization of discontinuities, as well as to the identification of physical properties, in order to predict the material behaviour.

In this particular case, the IP is solved in the form of a parameter estimation problem, in which the goal is the estimation of the characteristic acoustic impedance, transit time, and attenuation of each layer. These parameters are directly related to relevant material properties, such as the speed of sound, density, elastic modulus and elastic energy dissipation constants. The IP solution is obtained by minimizing a cost functional formulated as the least squares error between the waveform calculated using an equivalent model, and the measured waveform obtained from ultrasonic transmission tests.

The applied methodology allowed the accurate estimation of the desired parameters in materials composed of up to three layers. As a second contribution, a power law frequency dependence of the wave attenuation was identified for several homogeneous materials, based on the same ultrasonic transmission experiments.

© 2015 Elsevier B.V. All rights reserved.

1. Introduction

This paper presents a methodology to characterize layered materials solving an Inverse Problem (IP), based on an idealized model of the physical problem and using data obtained from ultrasonic wave transmission measurements.

Layered materials are a particular sort of composites, where the layers can be made of homogeneous materials, like polymers, metals or ceramics, or can be composed of fibber or particle reinforced materials [1,2]. In the course of time, more and more applications require the use of composites, which combine different materials properties in order to fulfil specific characteristics. Therefore, the study of composite materials is of great importance for the evaluation of their performance and for monitoring their properties.

Structures that can be studied like layered materials can be also found in nature. Rocks, dental pieces, bones, or other biological tissues (skin, fat, muscle) [3,4] are examples of these structures. In particular, in the case of biological tissues the detection and localization of the mechanical changes that suffer the structure when affected by pathology are the basis of many diagnosis tools.

Some methods widely used to identify material properties usually involve destructive testing, such as film indentation [5] or tensile tests [6], from which the values of the elastic constants can be inferred, based on the fitting to experimental curves. However, quantitative non-destructive evaluation (NDE) techniques are necessary to perform remote tests or whenever we need to assure the integrity of the analyzed piece, i.e., when the studied sample is on its service period or when it is a living tissue.

NDE techniques include, along with the selection of the measurement techniques, the experimental setup, the validation of physical models and the reliability of the computational methodology. The measurement technique chosen to carry out the tests in this work is ultrasound, high frequency acoustic waves capable to inspect both, solids or liquids. Ultrasound is used typically in the detection of defects, cracks, pores, or any lack of continuity in the sample. However, a more advanced use of this technique, since it involves a more sophisticated analysis of data, is the

* Corresponding author at: Department of Mathematics, Engineering School, National University of Mar del Plata, Mar del Plata, Argentina.

E-mail addresses: gmessineo@fi.mdp.edu.ar (M.G. Messineo), grus@ugr.es (G. Rus), elicabe@fi.mdp.edu.ar (G.E. Eliçabe), gfrontin@fi.mdp.edu.ar (G.L. Frontini).

identification of acoustical and mechanical properties of the material, the interest of this work.

Amongst the works that are based on ultrasonic NDE techniques, the determination of the acoustic impedance profile reported in [7] is one of especial interest. The data is the reflection impulse response of the ultrasonic wave, considering that the transducer response and the medium attenuation are known. The proposed application is the detection of plaque formation in the arteries using layered phantoms of liquid layers separated by thin polymeric membranes as test objects.

Ultrasound is frequently used to evaluate biological materials considered as layered structures. Leite et al. [8] perform a theoretical and computational study of ultrasonic wave propagation through three layers: fat, muscle and bone. This structure is of particular interest in therapeutic applications, especially at the interface muscle–bone, where excessive heating can occur during ultrasound therapy in soft tissues.

The complex nature of ultrasonic waves has led in recent decades to devote large amount of resources to study the theoretical and numerical aspects of the physical problem of wave propagation [9,10]. Methods to analyze and simulate the generation, propagation and interactions of a wave in a medium have been developed [11–13]. The Finite Element Method (FEM) or the Boundary Element Method (BEM), are proved and robust techniques that can be used to predict and visualize the wave propagation in structures with diverse geometry and complexity [14]. The limitation of these methods lies in the time required to process the code, related to the high resolution both, spatial and temporal, necessary to accurately represent the propagation of an ultrasonic wave.

Considering certain assumptions, the test to carry out the intended characterization can be well represented by equivalent models. In this paper, a model formulated in the frequency domain based on a transmission line (T-line) is used [15]. The model allows the determination of mechanical stresses at the interfaces of the samples, which using the electrical–mechanical analogies correspond to the electric tensions in a transmission line cascade. The same model was used in [16] to represent the propagation of an ultrasonic wave through a dental piece, composed by successive layers: enamel, dentin, pulp. The use of an equivalent model may be appropriate when it comes to optimize the computational resources. In this particular case, the transmission line model gives the possibility to represent the wave propagation through a layered material without numerically solving any differential equation. This feature provides an excellent computational efficiency. The disadvantage of these models is that they usually have restrictions that the real physical problems not always fulfil; therefore the obtained results may have errors.

Due to the complexity of the physical models that represent the studied situation it becomes necessary a direct comparison of the experimental data with the theoretical results, given by the solution of the so call forward problem. The IP provide a resolution framework for this sort of situations. Previous works have followed this approach. For instance, in [17] a method is presented to evaluate damage in Carbon Fibbers Reinforced Polymers (CFRP), which are widely used in industry, especially in aeronautics and automotive industries, due to its excellent relation weight-resistance. The evaluation is accomplished solving an IP to identify mechanical properties that allows monitoring the structural health of a piece for damage assessment or quality control. The datum is the waveform recorded at the end of the material in a transmission test [18,19], and the model used to represent the physical problem is an equivalent model based on the Transfer Matrix Formalism [20].

Hägglund et al. [21] carry out an integrity evaluation of an adhesive layer between two Pyrex dishes. They use an ultrasonic pulse-echo test, and the information contained in the measurements allowed obtaining a set of parameters from a maximum likelihood estimator.

Another application of ultrasound in biological tissues is found in [14], where Rus and García-Martínez dealt with the adhesion of nanostructured TiO_2 orthopaedic implants. An IP is solved to characterize the elastic modulus of each layer using FEM for the physical problem.

As addressed, the transmission line model is used in this work to represent the forward problem; the following two sections contain its description. Parameter estimation IP, formulated as the minimization of the least squares error between the experimental data and the theoretical functions obtained from the transmission line model, is introduced in Section 4. Also in this section, the proposed numerical resolution methodology based on one previously developed [22], is summarized.

In order to take into account the effect of wave attenuation, a thorough analysis performed based on the solution of the IP obtained using simulated measurements is reported in Section 5. In this section, the robustness of the methodology under modelling errors was also considered.

Finally, in Section 6 the inverse methodology was validated using experimental measurements. As a result, a set of parameters related to acoustic and mechanical properties of the layers of several materials could be identified.

2. The physical problem and the equivalent model

Ultrasound testing consists, generally, in recording the response generated by the propagation of an ultrasonic wave through a medium, either to detect discontinuities or to accomplish material characterization. Waves can take different modes, according to the particle oscillation direction and the wavefront geometry. A plane wave is one in which all the material particles oscillating in phase are on the same plane, and the oscillations can be longitudinal (P-wave) or transversal (S-wave) to the propagation direction.

P-wave propagation in an elastic, homogeneous, isotropic and non attenuating medium can be studied in one direction, and it is represented by the one-dimensional wave equation:

$$\frac{\partial^2 u(x,t)}{\partial x^2} = \frac{1}{c^2} \frac{\partial^2 u(x,t)}{\partial t^2}, \tag{1}$$

where $u(x,t)$ is the particle displacement and c is the speed of sound in the medium.

The proposed methodology to carry out the material characterization in this paper is based on an equivalent model which represents the propagation of P-waves, and allows obtaining the exact solution of the wave equation (Eq. (1)) in two points of a homogeneous material [15]. This model is derived from the electrical–mechanical analogies between voltage, V, and mechanical stress, σ, and between electric current, i, and particle velocity, v.

The equivalent model implies a significant idealization of the physical problem, since rarely waves present in the material are only P-waves. For instance, discontinuities or changes in consistency can affect the wave causing phenomena such as scattering, reflection, diffraction or mode conversion. Nevertheless, a variety of real situations can be well represented by this model, as we analyzed in a previous work [22]. We simulated the ultrasonic P-wave transmitted through a layered material using both, the equivalent model and FEM and evaluated the accuracy with which the equivalent model reproduces the physical problem. Furthermore, this comparison allowed verifying the improvement in the computational efficiency introduced.

A material composed by N homogeneous layers, of thickness d_i and density ρ_i, can be represented by a cascade connexion of N transmission lines (T-lines) as shown in Fig. 1, where
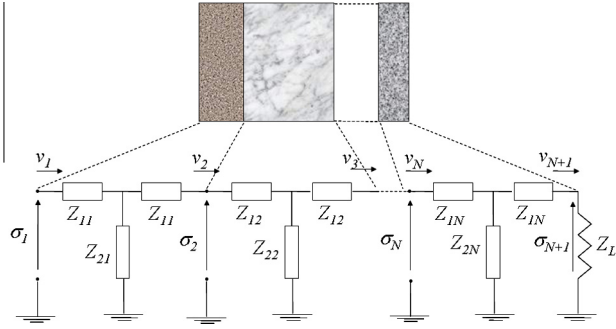
Fig. 1. N-layers material and its equivalent representation.

$$Z_{1i} = jZ_i \cdot \tan(\omega\tau_i/2)$$
$$Z_{2i} = -jZ_i/\sin(\omega\tau_i) \tag{2}$$

$Z_i = \rho_i c_i$ is the acoustic impedance of the i-th layer, $\tau_i = d_i/c_i$ is the corresponding wave transit time, and Z_L represents the acoustic impedance of the medium in contact with the end of the analyzed sample.

Mathematically, the model is represented by a matrix product relating the mechanical stress, $\sigma^*(\omega)$, and the particle velocity, $v^*(\omega)$, at one end of the material in terms of the same quantities at the other end. These functions are obtained as the Fourier transform of the temporal stresses and velocities, thus they are both in the frequency domain:

$$\begin{bmatrix} \sigma^*_{N+1}(\omega) \\ v^*_{N+1}(\omega) \end{bmatrix} = \prod_{i=N}^{1} \begin{bmatrix} \cos(k_i d_i) & -jZ_i \sin(k_i d_i) \\ -j\sin(k_i d_i)/Z_i & \cos(k_i d_i) \end{bmatrix} \begin{bmatrix} \sigma^*_1(\omega) \\ v^*_1(\omega) \end{bmatrix}. \tag{3}$$

In Eq. (3) the arguments of the trigonometric functions fulfil the relation $k_i d_i = \omega d_i c_i = \omega\tau_i$, where $k_i = \omega/c_i$ is the wave number of the material corresponding to the i-th layer and $\omega = 2\pi f$ is the angular frequency of the transmitted wave, with f in MHz.

The model parameters, Z_i y τ_i, drive to the calculation of the P-wave modulus, M, of each layer through the well known relation:

$$M_i = c_i^2 \rho_i = c_i^2 \frac{Z_i}{c_i} = \frac{d_i}{\tau_i} Z_i. \tag{4}$$

This modulus is defined as the ratio of the stress in the wave propagation direction, σ_{xx}, and the strain in the same direction, ε_{xx}, considering plane strain:

$$M = \frac{\sigma_{xx}}{\varepsilon_{xx}}, \tag{5}$$

and it is related to the Lamé parameters, λ y μ, as $M = \lambda + 2\mu$.

Usually, in order to characterize the elastic mechanical properties of a material, the tensile or Young modulus, E, is used, but this modulus is related to the P-wave modulus by Eq. (6),

$$M = \frac{E(1-v)}{(1+v)(1-2v)} \quad v : \text{Poisson relation.} \tag{6}$$

E is calculated measuring the speed of sound in rods or thin bars, where the material spreads out at right angles to the wave [23]. When the material has a breadth at least comparable to the wave length, it cannot move sideway and the propagation is faster than in a rod. This is the reason why the P-wave modulus is always larger than de Young modulus.

The main advantage of the equivalent model is that it offers the possibility of representing layered materials by doing a simple matrix product instead of numerically solve differential equations. The way in which the model is formulated makes unnecessary to discretize the sample and, consequently, it is more efficient than traditional numerical methods used to solve differential equations.

Due to the fact that the model is based on the one-dimensional wave equation (Eq. (1)), it has the limitation of representing only P-wave propagation problems. Modelling errors are introduced when this assumption is not fulfilled.

3. The extended model

Natural materials produce the weakening of the wave intensity as it propagates through the medium. This is a result of two causes: scattering and absorption, which can be combined in the concept of attenuation [24].

Scattering is the result of the inhomogeneity of the material, produced by grains, pores or other discontinuities where the acoustic impedance changes abruptly and therefore reflections at different angles are produced. This causes the dissipation of part of the energy and accordingly the transmitted amplitude of the wave looks attenuated. Absorption, on the other hand, is directly related to the losses of kinetic energy as the wave travels through the material. Amongst the processes that produce this effect it can be mentioned the viscous losses and the conversion of mechanical to caloric energy.

Under certain conditions, for some materials it may be reasonable to assume attenuation as a constant. However, in most of the media, included some liquids, biological tissues, rocks, as well as solid polymers, the ultrasonic wave attenuation shows a power law frequency dependence [25,26], an empiric law expressed as:

$$\alpha(\omega) = \alpha_0 \omega^\eta. \tag{7}$$

In Eq. (7), α_0 and η are two parameters that can be obtained by fitting experimental curves. The parameter η takes any value in the range [0:2].

In order to include the effect of attenuation in the model equations, a complex wave number, $\hat{k}$, has been considered:

$$\hat{k} = \frac{\omega}{c} - i\alpha(\omega), \tag{8}$$

where ω is the wave frequency, c is the speed of sound, and $\alpha(\omega)$ is the attenuation law.

When inserting the complex number $\hat{k}$ in Eq. (3), the trigonometric functions arguments become:

$$\hat{k}_i d_i = \left(\frac{\omega}{c_i} - j\alpha_i\right) d_i = \omega\tau_i - j\alpha_i d_i, \tag{9}$$

and it can be easily proved that the model representation is given now as:

$$\begin{bmatrix} \sigma^*_{N+1}(\omega) \\ v^*_{N+1}(\omega) \end{bmatrix} = \prod_{i=N}^{1} \begin{bmatrix} \cos(\omega\tau_i - j\alpha_i d_i) & \frac{-jZ_i}{\omega}\left(\omega - j\frac{\alpha_i d_i}{\tau_i}\right)\sin(\omega\tau_i - j\alpha_i d_i) \\ \frac{j\omega}{Z_i\left(\omega - j\frac{\alpha_i d_i}{\tau_i}\right)}\sin(\omega\tau_i - j\alpha_i d_i) & \cos(\omega\tau_i - j\alpha_i d_i) \end{bmatrix} \begin{bmatrix} \sigma^*_1(\omega) \\ v^*_1(\omega) \end{bmatrix}, \tag{10}$$

where the impedances of the i-th equivalent transmission line, Z_{1i} y Z_{2i}, are:

$$Z_{1i} = \frac{jZ_i}{\omega}(\omega - j\alpha_i c_i)\tan\left(\frac{(\omega - j\alpha_i c_i)\tau_i}{2}\right)$$
$$Z_{2i} = -\frac{jZ_i}{\omega}\frac{(\omega - j\alpha_i c_i)}{\sin((\omega - j\alpha_i c_i)\tau_i)} \tag{11}$$

and $\alpha_i = \alpha_{0i}\omega^{\eta i}$ according to Eq. (7).

4. The inverse problem

4.1. Formulation

The aim of this article, as stated, is the estimation of a set of parameters to characterize layered materials. Specifically, the

parameters we intend to find are acoustic impedance, transit time, and attenuation of each layer. This estimation will be the result of the solution of an Inverse Problem (IP) posed as the minimization of a functional expressed as the least squares error between experimental data and the waveforms predicted by the equivalent model (Eq. (10)). As the model is formulated in the frequency domain, the data are the Fourier transform of the measurements, which are the dynamic stresses registered at the end of the sample during a transmission test, denoted as σ_m^*.

Considering discrete data for K different frequencies, the cost functional is:

$$J(\mathbf{p}) = \frac{1}{K} \sum_{\omega_i = \omega_1}^{\omega_K} \left(\sigma_{N+1}^*(\mathbf{p}, \omega_i) - \sigma_m^*(\omega_i) \right)^2, \tag{12}$$

where $\sigma_{N+1}^*(\mathbf{p}, \omega_i)$ is the stress obtained from the equivalent model for each parameters vector and for each frequency. The parameters vector contains the acoustic impedance, the transit time and the attenuation of each layer, i.e., $\mathbf{p} = [Z_1 Z_2 \ldots Z_N \ \tau_1 \tau_2 \ldots \tau_N \ \alpha_{01} \alpha_{02} \ldots \alpha_{0N} \ \eta_1 \eta_2 \ldots \eta_N]$.

The minimization is carried out applying the Levenberg–Marquardt algorithm, suitable for non linear least squares problems [27].

4.2. Implementation issues

From de observation of Eqs. (3) and (10) it is clear the non-linear relation between the unknown parameters and $\sigma_{N+1}^*(\omega)$. Therefore, it is not possible to directly evaluate the existence and uniqueness of the least squares problem solution. We analyzed these features in a previous work [22] and developed an inverse methodology which allows determining the sought parameters in materials composed by non-attenuating layers. As a previous stage to the IP resolution, a detailed study of its characteristics was carried out, analyzing the uniqueness and stability of the solution.

Although in that work the optimal solution was determined to be unique, we detected the presence of many local minima. We concluded that, in order to accomplish the convergence of the minimization algorithm to the global minimum, it is necessary to properly initialize the transit time values. This is achieved by doing a previous estimation from the observation of the echoes in the measurements. The identification of this parameter is more feasible when we work with short-duration signals, i.e., wide bandwidth signals.

Contrarily, the complete ignorance of the values of the characteristic acoustic impedances does not implies an increase in the difficulty of solving the inverse problem; actually, from arbitrary initial values, the right solution was found.

As addressed, the acoustic transmission line model considers the relation between stresses and particle velocities at both ends of the sample. In order to solve the problem it is necessary to set the boundary conditions. At the end where the emitting transducer is placed, the boundary condition is the applied stress, σ_1. At the final end, the boundary condition is represented by Z_L, the acoustic impedance of the medium in contact with the sample. For real experiments, it is necessary to either be able of estimate the Z_L, or to measure it.

5. Simulated results

5.1. IP solution

In this section we analyze the IP solution for three samples, each one composed by three attenuating layers. The measurements were obtained simulating transmission tests (Fig. 2). The simulations were carried out based on the equivalent model and
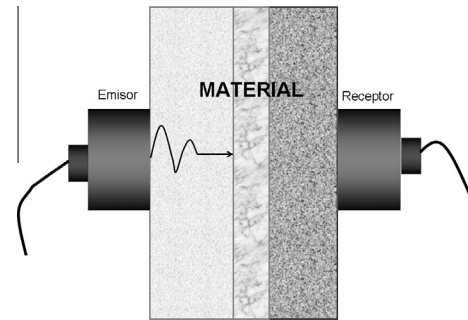

Fig. 2. Measurement scheme.

disturbing the so computed stress with additive gaussian noise having standard deviation $std_\varepsilon = 1\%$ and $std_\varepsilon = 5\%$ of the temporal simulated waveforms. The physical properties and the parameter values of the considered materials are shown in Table 1.

As a first step we assumed constant attenuation ($\eta = 0$). The excitation stress applied at the one end of the sample is shown in Fig. 3. The real and estimated values of the parameters are displayed in Table 2, where the subscripts indicate the order of the respective layer.

In Fig. 4, as an example, the cost functional evolution is shown for Material 2, for a given initial condition and for two different noise realisations. As can be seen, solutions converge.

The following step was the application of the inverse methodology for lossy materials, assuming that the attenuation follows a power law (Eq. (7)). Homogeneous as well as layered materials with 2, 3 and 4 layers were simulated. Some of the materials employed in these simulations are those used later in the experimental verifications. Their properties and parameter are shown in Table 3.

The stress displayed in Fig. 5 was used to excite the sample. Note that it has a central frequency near 5 MHz. The measurements were obtained, as in the previous cases, adding gaussian noise with different levels of standard deviation to the temporal computed stress.

The four parameters corresponding to each layer were estimated. It was found that the estimation errors increase with the number of layers. However, each layer parameters were estimated from arbitrary initial values of Z_i, α_{0i} and η_i with errors according to the noise level.

Fig. 6 illustrates, as an example, the estimated values of Alu-3 parameters vs. noise standard deviation using simulated measurements considering the homogeneous material, and when the Alu-3 sample is a layer of composites. It can be seen that for the homogeneous material, even with a high level of noise, the estimation of the parameters is good, while most significant errors are observed in the cases of 3 and 4 layers. In the same figure, the black line indicates the true value of the parameters.

5.2. Influence of modelling errors

As stated before, the equivalent model represents exactly the stresses at the interfaces of a sample because of the propagation of P-waves. When working with experimental data, the P-wave restriction is hardly fulfilled, since there are several causes that can provoke wave diffraction, scattering, mode conversion or a combination of these effects. As a consequence the wave front be no longer plane or the particles oscillations be no longer longitudinal, which implies that the model used in the proposed methodology does not represent exactly the equivalent data, introducing what is called modelling errors. As an example, in this work we studied cases where the interfaces are not perfectly parallel.

Table 1
Lossy materials for the simulated measurements.

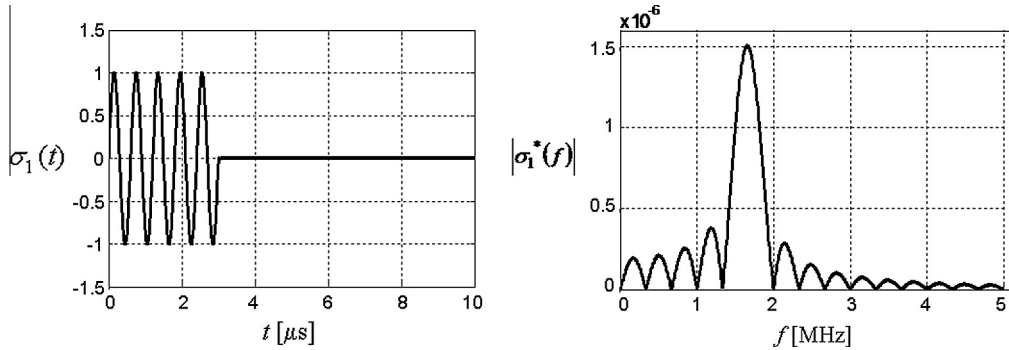|	Material 1			Material 2			Material 3		
	Enamel	Dentin	Pulp	Acrylic	Aluminium	Steel	Aluminium	HDPE	LDPE
ρ (kg/m^3)	3000	2000	1000	1190	2795	7870	2700	950	920
c (m/s)	6250	3800	1570	2654	6419	5960	6419	1124	1950
d (mm)	1.88	2.36	3.76	12.14	6.05	6.05	10	1	6
Z^v (MRayl)	18.75	7.6	1.57	3.16	17.94	46.90	17.33	1.07	1.79
τ^v (µs)	0.30	0.62	2.39	4.57	0.94	1.01	1.56	0.89	3.07
α^v (Np/m)	34.52	50.42	57.55	73.66	13.82	11.50	13.81	46.00	57.55

Fig. 3. Excitation stress 1 and its amplitude spectrum.

Table 2
Estimated and true parameters values in lossy material.

|		Z_1 (MRayls)	Z_2 (MRayls)	Z_3 (MRayls)	τ_1 (µs)	τ_2 (µs)	τ_3 (µs)	α_1 (Np/m)	α_2 (Np/m)	α_3 (Np/m)
Material 1	True	18.75	7.60	1.57	0.30	0.62	2.39	34.52	50.42	57.55
	Std$_\varepsilon$ = 1%	18.57	7.56	1.57	0.3007	0.6213	2.3949	33.83	50.76	60.08
	Std$_\varepsilon$ = 5%	14.77	6.14	1.61	0.3010	0.6209	2.3940	31.38	27.58	127.66
Material 2	True	3.16	17.94	46.90	4.57	0.94	1.01	73.66	13.82	11.50
	Std$_\varepsilon$ = 1%	3.13	17.85	46.85	4.5744	0.9427	1.0149	73.85	13.80	11.60
	Std$_\varepsilon$ = 5%	3.01	17.49	46.59	4.5750	0.9433	1.0140	74.55	13.73	11.93
Material 3	True	17.33	1.07	1.79	1.56	0.89	3.07	13.81	46.00	57.55
	Std$_\varepsilon$ = 1%	17.32	1.07	1.79	1.5579	0.8897	3.0768	13.81	48.10	57.22
	Std$_\varepsilon$ = 5%	17.27	1.07	1.79	1.5579	0.8898	3.0764	13.79	56.80	55.87
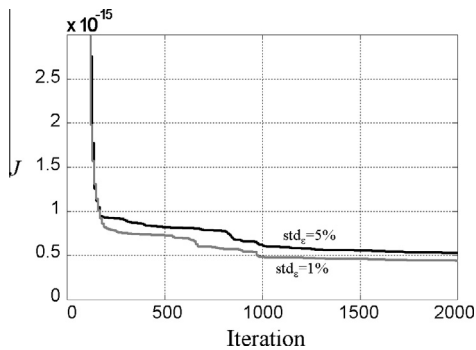
Fig. 4. Functional evolution with different levels of noise in Material 2.

The proposed methodology was based on the assumption that the layers are in perfect contact. However, this can be not true due to the lack of adhesion or to the presence of cracks on the wave path. These imperfections cause a reduction on the amplitude of the transmitted wave dependent on the thickness of the discontinuity and on the wave frequency [23]. Even when the gap filled with air or liquid is a few microns wide, it introduces significant errors in the estimates. We analyzed the effect of this kind of modelling error using simulated experiments.

5.2.1. Non-parallel interfaces

The transmission line model is suitable to represent without errors materials with perfectly plane and parallel interfaces. When this requirement is not fulfilled, the usage of the model to predict the transmitted waveform entails modelling errors.

The effects caused by these errors, are illustrated making use of some particular cases where the interfaces are plane but not parallel, and consequently the wave suffers diffraction and mode conversion. The considered geometries are shown schematically in Fig. 7 for three different cases (A: $\beta = 1.14°$; B: $\beta = 2.52°$; C: $\beta = 1.14°$).

The layers of the simulated samples are assumed to be the same as those in Material 1 and the excitation stress is that displayed in

Table 3
True values of the parameters of the simulated attenuating materials.

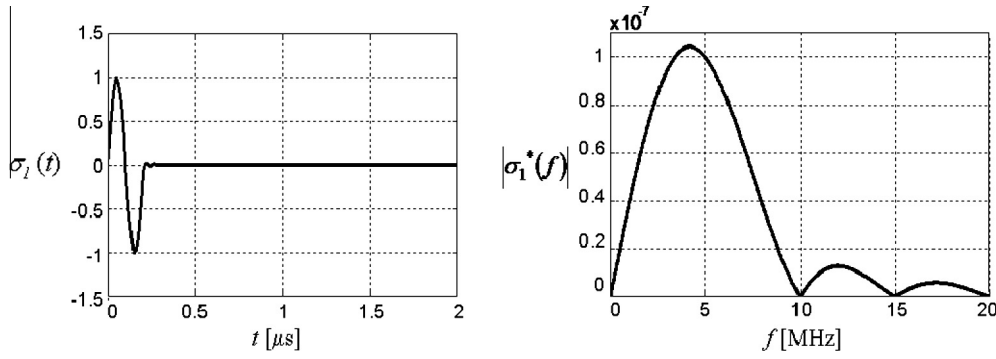|	Aluminium (Alu-3)	Acrylic (Acr-3)	Aluminium (Alu-10)	Acrylic (Acr-10)
Z^v (MRayl)	17.87	3.05	17.01	3.19
τ^v (µs)	0.64	1.15	1.57	3.73
α_0^v	1.56e^{-4}	1.22e^{-2}	8.10e^{-3}	8.18e^{-4}
η^v	0.78	0.54	0.49	0.67
α (Np/m) ($f = f_c$)	109.9	136.4	38.2	86.3

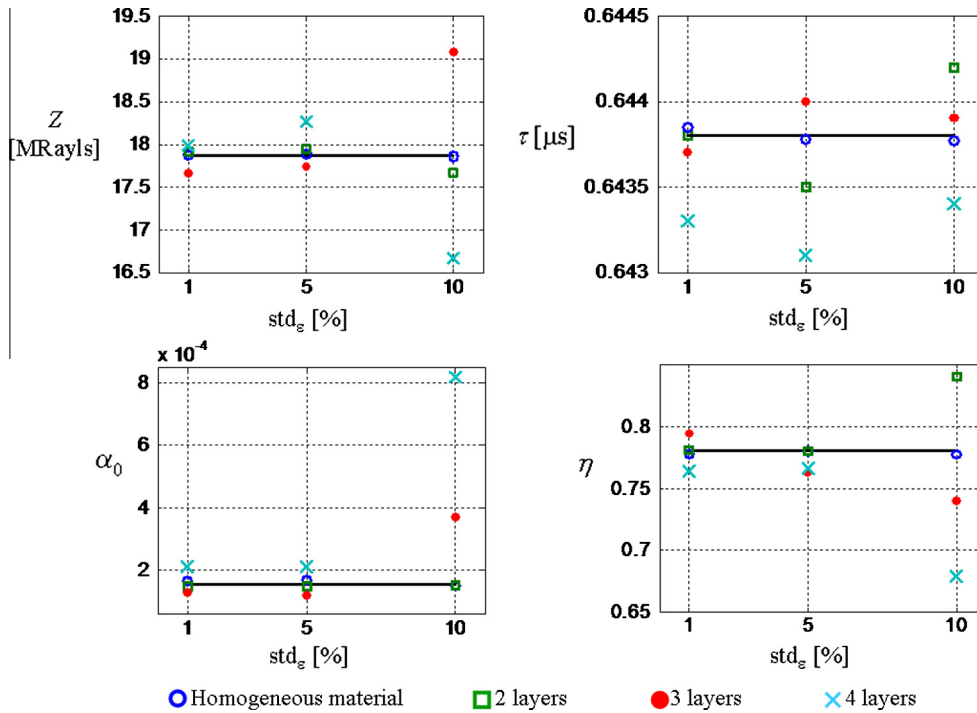**Fig. 5.** Excitation stress 2 and its amplitude spectrum.

Fig. 6. Estimated values for Alu-3 as a homogeneous material and as part of a composite of 2, 3 and 4 layers.
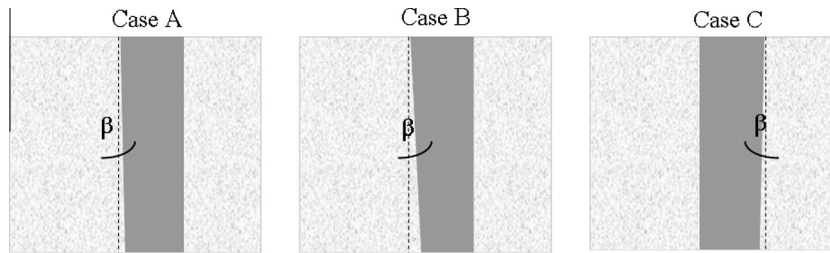

Fig. 7. Material with non-parallel interfaces.

Fig. 3. The transmission experiment was simulated using the true values of all the parameters with the exact model represented by the Eq. (1) solved using FEM. The obtained stress function is different from the one calculated using the idealized model as could be expected and both amplitude spectra are illustrated in Fig. 8.

The IP was solved based on the equivalent model using as data the simulated experiments. Table 4 shows the estimated parameters values. Even when it can be seen that errors are more significant than when there is no modelling error, the obtained values are good approximations and give useful information about the acoustic impedances of each layer.

5.2.2. Fluid trapped at the interfaces

Another cause of modelling error is the fact that eventual and uncertain presence of fluid (water, air, coupling gel) in the sample interfaces was not taken into account in the model used to solve the IP. A very thin gap, even a micrometric one, diminishes the wave transmitivity between layers, which could lead to wrong
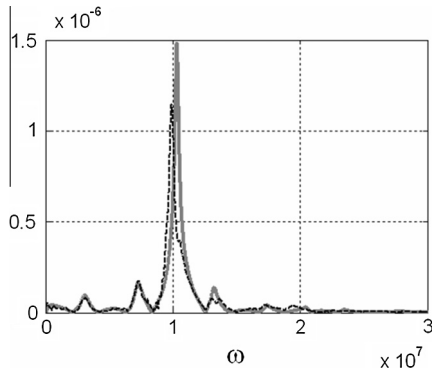
Fig. 8. Comparison of amplitude spectra with modelling error (black) and without modelling error (grey).

Table 4
Estimated parameters in materials with non-parallel interfaces.

		Case A	Case B	Case C
Material 1	Z_1 (MRayl)	19.1760	20.5590	18.9920
	Z_2 (MRayl)	6.6468	7.2173	6.9716
	Z_3 (MRayl)	1.4750	1.4750	1.3979
	τ_1 (μs)	0.3206	0.3271	0.3103
	τ_2 (μs)	0.6343	0.6105	0.6300
	τ_3 (μs)	2.4449	2.3712	2.5140
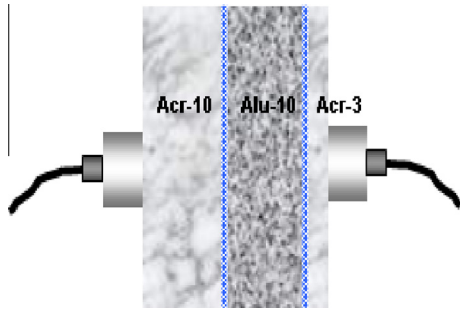
Fig. 9. Simulated scheme with water at the interfaces.

Table 5
Physical properties of water.

c (m/s)	ρ (kg/m^3)	d (μm)	α_0	η
1650	1002	10	5.4967e^{-15}	2

Table 6
Parameter values.

		True	Estimated	
			With modelling errors	Without modelling errors
Acr-10	Z_1 (MRayls)	3.195	3.192	3.153
	τ_1 (μs)	3.724	3.736	3.724
	α_{01}	8.18e^{-4}	9.6e^{-4}	1.02e^{-3}
	η_1	0.6660	0.6568	0.6532
Alu-10	Z_2 (MRayls)	17.009	17.383	16.849
	τ_2 (μs)	1.566	1.563	1.566
	α_{02}	8.10e^{-3}	1.53e^{-2}	6.7e^{-3}
	η_2	0.4863	0.4474	0.4972
Acr-3	Z_3 (MRayls)	3.052	3.026	3.075
	τ_3 (μs)	1.148	1.159	1.148
	α_{03}	1.22e^{-2}	4.76e^{-4}	1.13e^{-2}
	η_3	0.5387	0.7341	0.5446

parameter estimation. To study this effect, the situation illustrated in Fig. 9 was simulated, where the sample is composed by Acr-10, Alu-10 and Acr-3 (Table 3), and layers of water with a thickness of 10 μm were intercalated at the interfaces. The considered values of water properties are in Table 5. Then, the IP was solved assuming the material layers in perfect contact.

The estimated parameters values are shown, along with the true ones and the values estimated without modelling errors in Table 6. We observe that attenuation parameters are much more sensitive to this kind of modelling errors than acoustic impedances and transit times.

The curves representing the power law $\alpha(\omega) = \alpha_0\omega^{\eta}$ for the estimated and the true values of the parameters are depicted in Fig. 10. It can be seen that, since the error in the estimation of the layers parameters is larger as the corresponding layer is farthest from the excitation stress, then the adjustment of the curves is worst for the farthest layer. In order to verify the generality of this assertion, the same case was simulated in opposite sense, i.e., from Acr-3 to Acr-10. The curves obtained with the estimated parameters are shown in Fig. 11.

6. Experimental results

6.1. Materials and experimental setup

The inverse methodology discussed previously was applied to the material characterization of real samples using data obtained from ultrasound tests. The transmission tests were performed on samples composed by various materials. The analyzed samples are formed by disks of metals and acrylic, which have been carefully mechanized in order to avoid surface roughness and get as perfect as possible parallel interfaces. The measurements were first taken on the isolated disks, and then on arrays composed by stacked disks.

Two experimental configurations were used for recording data. The first one, named as Configuration I, is displayed in Fig. 12 and it involves the testing of a stack of disks joined by simple contact with transducers coupled with oil. The electrical excitation signal applied to the transducers is a 100 V pulse of nominal frequency 7.5 MHz, although the measured central frequency is near 5 MHz.

The oil layer necessary for coupling transducers to material can usually cause problems in this sort of experiments, since it is not possible to control its thickness and homogeneity. An alternative to avoid this obstacle is provided by immersion measurements in a water tank. In Fig. 13 we show this kind of experimental setting, which we call Configuration II. The sample is immersed in a water tank with an unfocused piezoelectric transducer acting as emitter. As receptor, a hydrophone was used separated 124 mm from the
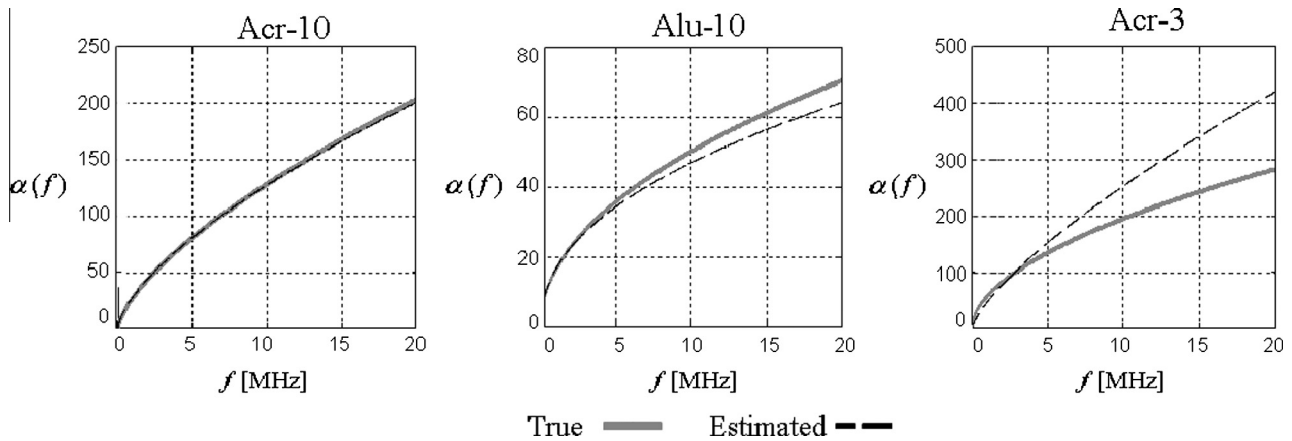
Fig. 10. True and estimated attenuation curve with modelling error, transmitting from Acr-10 to Acr-3.
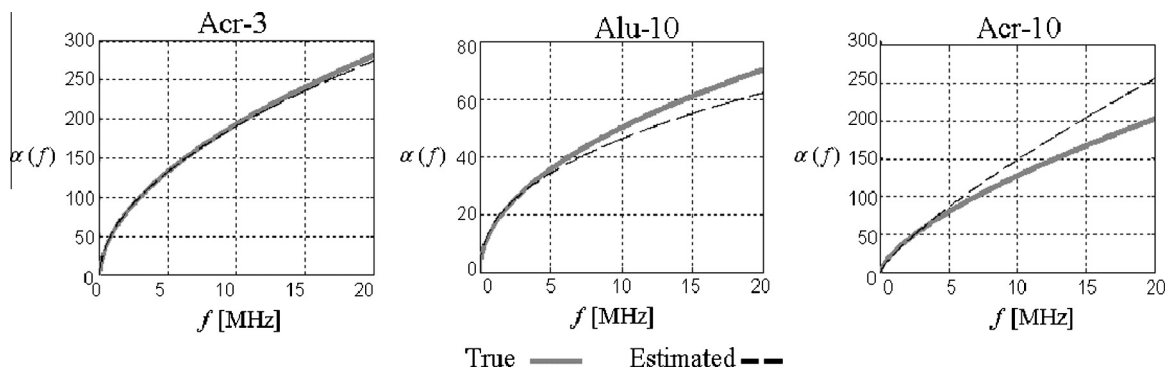

Fig. 11. True and estimated attenuation curve with modelling error, transmitting from Acr-3 to Acr-10.

Fig. 12. Configuration I with transducers in contact with the sample.
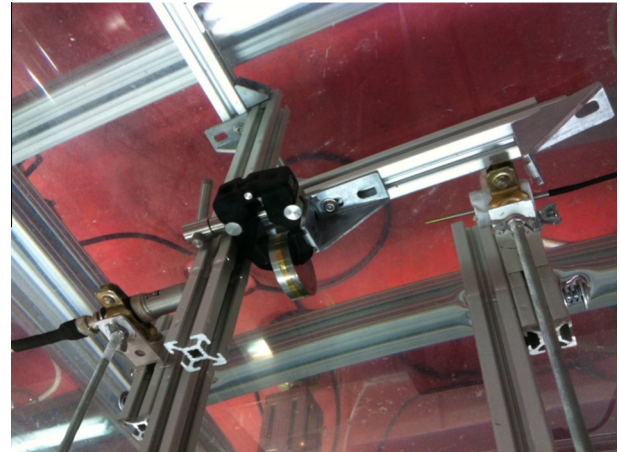

Fig. 13. Configuration II in immersion tank.

transmitter, and the sample was located at the middle point. The disks were held together by linear clamps, applied the nearest possible to the site of measurement in order to avoid the water to remain trapped in the interfaces, which can greatly influence the data. In this case, the electrical signal is a cycle of a sine, 8 Vpp, amplified 40 dB with central frequencies 5.5 and 6 MHz, and the received signal is amplified 37.5 dB. The sample was explored on a 2 square millimetres plane, parallel to the face of the material and in 3 steps of 1 mm on each direction, permitting to obtain 9 measurements per sample. This allows averaging the signals or the estimations obtained at working with each measurement.

The latter configuration avoids some errors caused by the coupling layer when transducers are in contact with the sample, and also allows focusing the ultrasound wave. However, this setting is possible only in a laboratory test, while Configuration I can be applied to pieces in service.

As a first step, we performed a direct characterization of the homogeneous disks. The description of these materials is given by the mechanical, acoustical and physical properties measured on each disk and the true parameter values: acoustic impedance and transit time. The samples are 40 mm diameter, cylindrical, and they were weighted and measured in order to determine its

Table 7
Materials evaluated using Configuration I.

Material	d (mm)	ρ (kg/m^3)	c (m/s)
Steel (Ace-10)	9.67	7821	5964.24
Acrylic (Acr-14)	14.39	1180	2731.90

thickness, d, and density, ρ. Furthermore, from the transit time observed in the ultrasound measurements the speed of sound in the material, c, was calculated.

Table 7 shows the obtained results for the disks to be used in Configuration I.

For Configuration II, different samples were used, whose thickness and mechanical and physical properties are in Table 8.

The samples named Acr-10 and Acr-14 are made out of the same type of acrylic, while Acr-3 corresponds to a different one. The discrepancy in the values of ρ and c for different samples of the same type of material can be attributed to the fact that the measurements were made at different times and under different environmental conditions.

The properties shown in Tables 7 and 8 are related to the parameters of interest by the following equations:

$$Z = \rho c$$
$$\tau = d/c ,$$
(13)

whose values are listed, along with the longitudinal wave modulus, $M = c^2\rho$, in Table 9, and they are considered as the true ones in this paper. In all cases, the cells with two values indicate the corresponding to measurements done with different central frequency transducers (f_c = 5.5 MHz and f_c = 6 MHz) in Configuration II.

The identification of acoustic attenuation and its relation with frequency is important when it comes to characterize a material, since neglecting its influence, which in many cases is important,

Table 8
Materials evaluated using Configuration II.

Material	d (mm)	ρ (kg/m^3)	c (m/s)
Acrylic 3 (Acr-3)	2.61	1168	2613;2614.4
Acrylic 10 (Acr-10)	9.98	1190	2685;2685.2
Aluminium 3 (Alu-3)	3.79	2876	6213.1;6213.1
Aluminium 10 (Alu-10)	9.90	2663	6387.1;6387.1

Table 9
True value of parameters and elastic modulus.

Material	Z^v (MRayls)	τ^v (μs)	M^v (GPa)
Ace-10	46.65	1.622	278
Acr-14	3.22	5.27	8.80
Acr-3	3.052;3.054	0.999;0.998	7.97;7.98
Acr-10	3.195;3.196	3.717;3.716	8.58;8.58
Alu-3	17.87	0.61	111.02
Alu-10	17.01	1.55	108.64

can increase the errors in the estimation of the rest of the parameters. A study of the attenuation was carried out by using the inverse methodology.

For a great variety of materials, values of attenuation are available in bibliography, although its dependency with frequency is not always documented, and the tabulated values are valid for a small range of frequencies and must be considered just as typical values.

Furthermore, polymeric materials such as acrylic have properties which depend on its molecular weight, the additives incorporated during manufacture and temperature of measurement. Even in metals, theoretical values of attenuation are approximated, and they are influenced by the tempering process, which determines the texture, the grain size, the residual stresses and the hardness. The ageing and the exposure to certain factors could modify materials properties and may also cause variations in the attenuation.

Traditional ultrasound methods to measure attenuation involve the temporal signals propagated through the material. These methods are based on the comparison of relative amplitudes between successive reflections, or between emitted and received wave in measurements made on different thickness samples, and using different frequencies [28]. From these measurements, experimental attenuation curves as a function of frequency are obtained, and for a wide range of materials those curves are well fitted by the power law of Eq. (7). The methodology developed in this paper uses a single transmission measurement to obtain α_0 and η simultaneously with Z and τ.

On the other hand, we have mentioned that Z_L, the acoustic impedance in contact with the final end of the sample, cannot be estimated as a model parameter. The determination of the value of Z_L was done simultaneously with the estimation of α_0, solving de IP for every sample, with the true values of Z and τ, and a fixed value for η. Table 10 shows the estimated values of α_0 and Z_L for some of the disks, considering two cases, in which the wave is attenuated according to a constant ($\eta = 0$) and a linear ($\eta = 1$) attenuation law, respectively. For each sample, the values of Z_L obtained are the same with both models of attenuation, and in all cases they are close to 2 MRayls.

The attenuation values in Table 10 are just a first estimation, and α considering constant attenuation is comparable to the one estimated for the central frequency, f_c, assuming linear attenuation.

Once the disks were individually characterized, the IP was solved in order to determine the parameters values of homogeneous materials and also of samples composed by two and three layers, which were measured in both ways of propagation to prove the repeatability of the results.

When working with experimental measurements, we should deal with the IP own obstacles, especially the presence of local minima and the difficulty of determining Z_L, and also with measurement errors, which are impossible to quantify. Amongst these errors we can mention the misalignment of transducers or, in Configuration I, the effect of the coupling medium between the

Table 10
Values of α_0 y Z_L obtained from solution space, with Z^v y τ^v.

Material	$\eta = 0$	$\eta = 1$		Z_L (MRayls)
	$\alpha = \alpha_0$ (Np/m)	α_0	$\alpha = \alpha_0 2\pi fc$ (Np/m)	
Ace-10	12.5	3.5e−7	12.09	1.9
Acr-14	116.5	3.4e−6	117.49	2
Acr-3	165;176	4.56e−6;4.65e−6	157.58;175.30	1.96
Acr-10	87.2;90.8	2.3e−6;2.3e−6	79.48;86.70	2.25
Alu-3	82.3;84.1	2.28e−6;2.26e−6	78.79;85.20	1.84
Alu-10	54.5;55.7	1.4e−6;1.38e−6	48.38;52.02	2.1

transducers and the sample, which is inhomogeneous, of unknown thickness, and increases the measurement noise. Moreover, the modelling errors mentioned in Section 6 are present, as the material layers are not in perfect contact, and possibly air or water may be trapped at the interfaces.

6.2. Homogeneous materials

The IP was solved to estimate all the parameters that characterize the sample, $\mathbf{p} = [Z \ \tau \ \alpha_0 \ \eta]$. The data were the measurements of an ultrasonic wave transmitted through the sample, and they are compared to the theoretical waveforms obtained from the equivalent model, by solving the functional in Eq. (12).

We obtained the initial values of τ from the observation of temporal measurements. This requires the analysis of the waveform to be made by an operator with rigorous training in ultrasound. Otherwise, the values of α_0, η and Z were initialized arbitrarily. In all cases the algorithm converged to the global minimum and the sought parameters were estimated with very low error. The results displayed in Table 11 were found with Z_L as in Table 10.

Regarding attenuation, in many metals its dependence with frequency is linear, at least in a range of the spectrum. In Table 11 it is shown that the value of η for steel is nearly 1. In the case of aluminium, the values estimated for the two samples are quite different, and this can be related with the modelling errors in Alu-3 due to neglecting the shear waves originated in the faces of the samples which are parallel to the wave propagation. On the other hand, the curves of attenuation for the samples Acr-14 and Acr-10, both made using the same type of acrylic, are almost coincident, while Acr-3 is much more attenuating. The curves displayed in Fig. 14 were obtained solving Eq. (7) with the estimated parameters for the three acrylic samples.

In Fig. 15 the waveforms recorded using Configuration I (grey) are plotted, along with the calculated (black) using the estimated parameters, while Fig. 16 shows the ones corresponding to the experiments made with Configuration II. For the calculated waveforms, the pulse used as the excitation signal for the equivalent model, is that obtained as the output of a test carried out with no sample, as reported in a previous work [29].

The waveforms obtained using Configuration I are noisy; nevertheless the error in the estimations is low and the fitting to the experimental curves is acceptable.

The accurate values of the parameters obtained from the resolution of the IP using the measurements recorded with Configuration II result in a very good fitting to the experimental waveforms, especially for acrylic (Fig. 16).

In the measurement registered for the Alu-3 sample, additional reflections are observed. These reflections are caused by the shear waves originated by mode conversion, which are not considered by the equivalent model, since it represents only the propagation of longitudinal waves.

6.3. Two layers materials

For solving the IP in layered materials, only measurements obtained using Configuration II were used. As the materials are
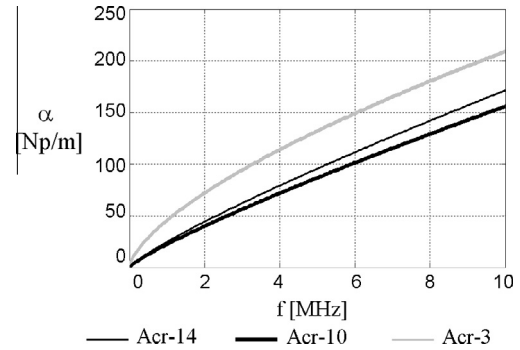

Fig. 14. Attenuation as a function of frequency in acrylic.

joined by simple contact, the gap in the interfaces may be filled with water and, as mentioned before, this could greatly influence the parameters estimation.

On the other hand, when the samples are composed by metals, which are less attenuating, also the error caused by mode conversion is present. This effect was already quoted for homogeneous materials. The shear wave generated at the edges of the sample propagates to the neighbouring layers, and its successive reflections arrive to the receptor. This could be considered as another modelling error, since the equivalent representation of the experimental setup utilized in this paper does not consider shear wave propagation. Therefore, as the number of layers increases we can expect errors to increase.

We considered samples composed by two layers, acrylic and aluminium, and take measurements using the transducer with central frequency $f_c = 5.5$ MHz. In this case, the solution of the IP is $\mathbf{p} = [Z_1 \ Z_2 \ \tau_1 \ \tau_2 \ \alpha_{01} \ \alpha_{02} \ \eta_1 \ \eta_2]$. Tables 12a and 12b show the values of the parameters that could be estimated (Z and τ) and the properties calculated from them (c, ρ and M). As can be seen, the estimations are in good agreement with the true values calculated for the homogeneous materials (Table 9).

We found that the estimates of characteristic acoustic impedances are sensitive to the value of Z_L, which as explained before cannot be precisely determined. Therefore, the uncertain Z_L value is another source of error. However, this value does not affect the estimations of transmission (T) and reflection (R) coefficients at the interfaces between the layer i and the layer $i + 1$, given by:

$$T_{i,i+1} = \frac{2Z_{i+1}}{Z_{i+1} + Z_i}; \quad R_{i,i+1} = \frac{Z_{i+1} - Z_i}{Z_{i+1} + Z_i}. \tag{14}$$

Table 13 contains the estimated coefficients, T_e and R_e, which are the same for different values of Z_L; as can be observed they are very close to the true ones, T^v and R^v, that were computed taking the parameter values reported in Table 9.

Regarding the attenuation parameters, α_0 and η, well estimated for homogeneous materials as reported before (Table 10), we must say that we were not able to identify them for layered materials. A possible justification of this fact is the possible trapped fluid at the interfaces analyzed in Section 5. However, the values of α_0 y η obtained from the IP solution are to be considered as adjustment

Table 11
Homogeneous materials estimated parameters.

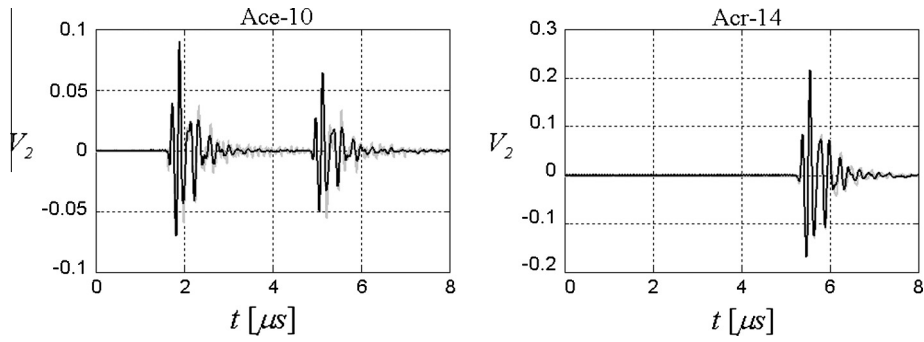| Material	Z (Mrayls)	τ (μs)	α_0	η	α (Np/m) f = fc	c (m/s)	ρ (kg/m³)	M (GPa)
Ace-10	46.68	1.623	6.93e−7	0.9587	11.69	5958.5	7834.2	278.14
Acr-14	3.10	5.280	4.53e−5	0.8435	95.48	2725.4	1137.5	8.45
Acr-3	3.11	0.988	1.43e−3	0.6623	140.64	2640.1	1178.0	8.21
Acr-10	3.16	3.722	3.85e−5	0.8473	93.94	2681.0	1178.5	8.47
Alu-3	17.37	0.614	7.01e−5	0.8087	87.52	6172.6	2814.0	107.22
Alu-10	17.10	1.540	6.01e−4	0.6295	33.45	6426.9	2661.4	109.93

Fig. 15. Experimental measurements (grey) and waveforms calculated with the model (black) with parameters values estimated using Configuration I.
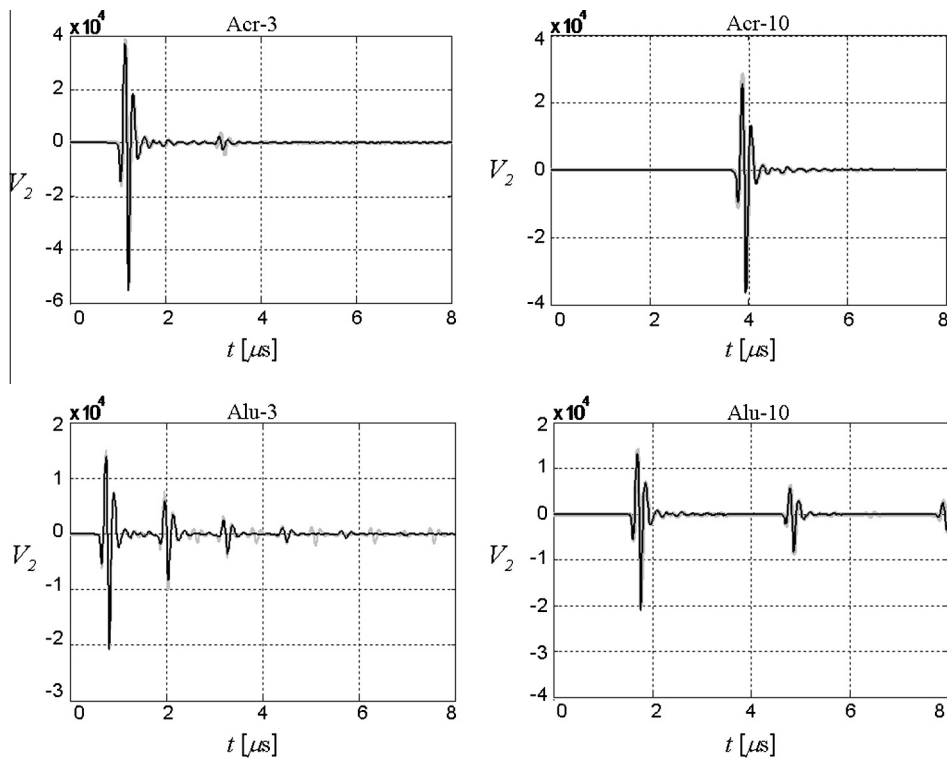

Fig. 16. Experimental measurements (grey) and waveforms calculated with the model (black) with parameters values estimated using Configuration II.

Table 12a
Estimated parameters for acrylic in 2 layers materials.

Acr-3	True	Estimated		Acr-10	True	Estimated	
		Acr-3/Alu-10	Alu-10/Acr-3			Acr-10/Alu-10	Alu-10/Acr-10
Z (MRayls)	3.11	3.16	2.96	Z (MRayls)	3.16	3.18	2.91
τ (µs)	0.99	0.99	0.99	τ (µs)	3.72	3.73	3.73
c (m/s)	2640.10	2643.30	2635.80	c (m/s)	2681.00	2655.40	2673.00
ρ (kg/m^3)	1178.00	1196.50	1121.50	ρ (kg/m^3)	1178.50	1197.90	1089.20
M (GPa)	8.21	8.36	7.79	M (GPa)	8.47	8.45	7.78

Table 12b
Estimated parameters for aluminium in 2 layers materials.

Alu-10	True	Estimated			
		Acr-3/Alu-10	Alu-10/Acr-3	Acr-10/Alu-10	Alu-10/Acr-10
Z (MRayls)	17.10	16.54	17.33	17.69	16.97
τ (µs)	1.54	1.53	1.53	1.55	1.55
c (m/s)	6426.90	6447.40	6447.80	2748.00	6437.90
ρ (kg/m^3)	2661.40	2566.20	2687.70	6440.00	2636.30
M (GPa)	109.93	106.67	111.74	113.97	109.26

Table 13
Comparison of reflection y transmission coefficients.

Material	T^v	T_e	R^v	R_e
Acr-3 Alu-10	1.69	1.68	0.69	0.68
Alu-10 Acr-3	0.30	0.29	−0.70	−0.71
Acr-10 Alu-10	1.68	1.69	0.68	0.69
Alu-10 Acr-10	0.32	0.29	−0.68	−0.71

values, permitting an accurate convergence of the rest of the sought parameters.

The acoustic impedance values and the transit time obtained solving the IP are near the true ones although, as expected, they have larger errors than the obtained in homogeneous materials, but still remain in acceptable values, making clear the robustness of the methodology.
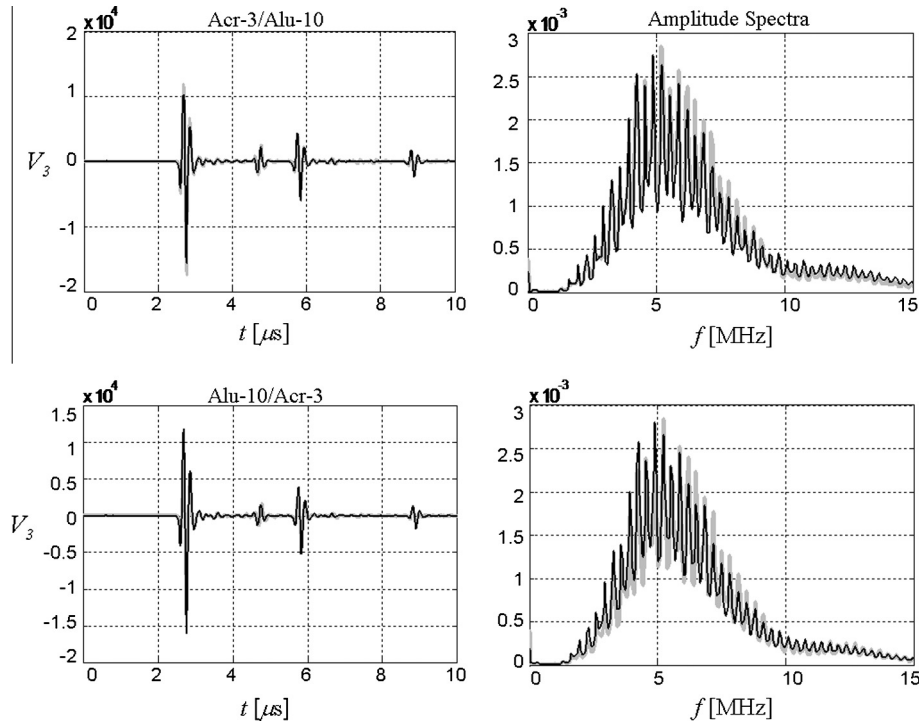
Fig. 17. Experimental waveforms (grey) and calculated by the model (black) with estimated parameters in samples of Acr-3 and Alu-10.
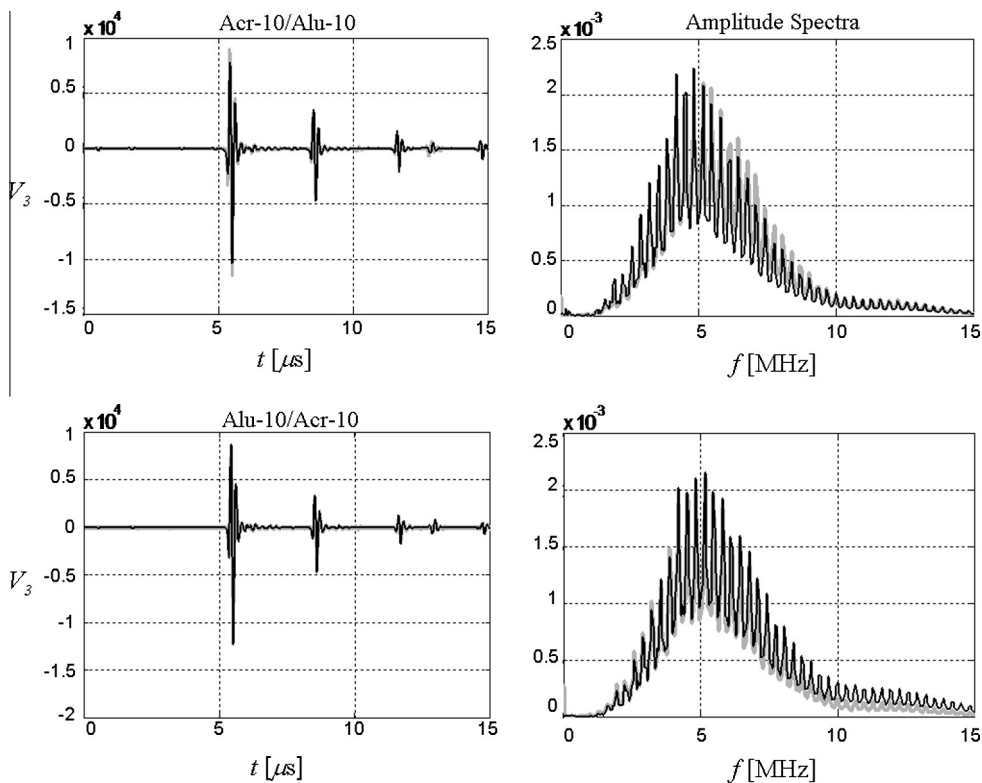

Fig. 18. Experimental waveforms (grey) and calculated by the model (black) with estimated parameters in samples of Acr-10 and Alu-10.

Table 14
Parameters estimated in 3 layers materials.

	True	Estimated	
		Acr-3/Alu-10/Acr-10	Acr-10/ Alu-10/Acr-3
Acr-3			
Z (MRayls)	3.16	3.39	3.54
τ (μs)	0.99	1.00	1.02
c (m/s)	2643.30	2599.08	2569.91
ρ (kg/m³)	1196.50	1305.30	1378.18
M (GPa)	8.36	8.82	9.10
Alu-10			
Z (MRayls)	17.10	16.87	18.69
τ (μs)	1.54	1.55	1.55
c (m/s)	6426.90	6388.33	6386.27
ρ (kg/m³)	2661.40	2640.18	2927.36
M (GPa)	109.93	107.75	119.39
Acr-10			
Z (MRayls)	3.16	3.07	2.85
τ (μs)	3.72	3.72	3.72
c (m/s)	2681.00	2683.59	2685.39
ρ (kg/m³)	1178.50	1144.66	1060.62
M (GPa)	8.47	8.24	7.64

The waveforms of the experimental measurements and the corresponding amplitude spectra are plotted in Figs. 17 and 18, along with those recorded using the estimated parameters (Table 12). It can be seen that the equivalent model represents accurately the wave propagation through the materials composed by 2 layers.

6.4. Three layers materials

The methodology was tested also in samples composed by three layers of acrylic and aluminium (Acr-3, Alu-10 and Acr-10), recording the transmission from Acr-3 to Acr-10 and reversely. For both cases, the estimated values of parameters Z and τ are shown in

Table 14, as well as the properties calculated from that estimates, c, ρ and M. Again, the subscripts indicate the layers sequence. In this case the errors are more important than in the estimations of 2 layers materials, as could be expected. However, the recovered waveforms show a good fitting to the experimental ones, as shown in Fig. 19.

7. Conclusions

An inverse methodology has been developed in this paper to characterize layered materials. The main goal is the identification of a set of parameters related to acoustical, physical and mechanical properties of the studied sample. Particularly, the speed of sound, density, elastic P-wave modulus and attenuation of each layer are obtained.

A parameter estimation IP was solved minimizing a cost functional posed as the least square error between the experimental data and the waveforms calculated by means of an equivalent model representing the physical problem. The data came from ultrasonic transmission tests, carried out using two different configurations.

An equivalent model suited to represent the wave propagation through an elastic medium takes the form of an electric transmission line, based on electrical–mechanical analogies and formulated in the frequency domain. The forward solution of this problem, represents exactly the mechanical stresses generated by a P-wave propagation at the interfaces of the sample. Thus, the numerical solution of the exact model using finite elements is unnecessary, improving significantly the computational efficiency. This benefit is multiplied when facing the IP, since it requires the repeated solution of the forward problem.

The equivalent model used was presented in the literature by other authors for non attenuating materials. Since real materials usually produce intensity losses, the effect of attenuation should be taken into account. This can be accomplished including in the
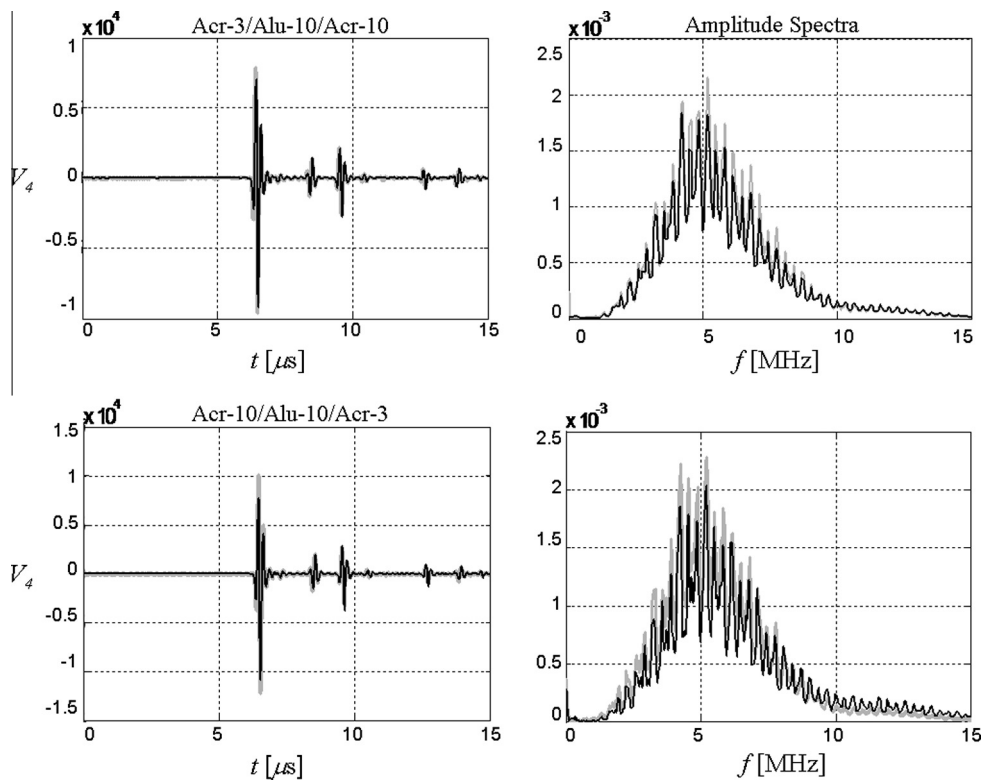

Fig. 19. Experimental waveforms (grey) and calculated by the model (black) with estimated parameters in samples of Acr-3, Acr-10 and Alu-10.

equivalent model equations a complex wave number having an attenuation law which holds a potential relation with frequency.

The parameters identified solving the IP with simulated data are the characteristic acoustic impedance, the transit time and the attenuation corresponding to each layer. Their errors in the estimations stay within an acceptable range.

The methodology proposed and analyzed in this work was validated carrying out ultrasound transmission tests. The experimental measurements had to be properly processed to be used as data for the resolution of the IP.

First, we were able to accurately estimate all parameters on homogeneous materials, obtaining errors below 10% in the values of acoustic impedances and transit times. As a second contribution of this work, the parameters corresponding to an attenuation frequency power law were identified.

Layered materials are the main interest of this paper. For these cases we found that the attenuation parameters cannot be identified, as a consequence of the modelling error incurred when neglecting the effect of the fluid trapped at the interfaces. However, we conclude that the methodology is robust, since it allows the right identification of the acoustic impedances and the transit times, and as a consequence, good estimates of P-wave modulus could be obtained.

It is relevant to mention that best fitting to the experimental curves is obtained when materials are strongly attenuating, such as acrylic. In measurements done on metals appear reflections originated by shear waves due to mode conversion at the edges, which are not represented by the model. Also, the model provides a better fitting in cases of thicker layers.

It can be highlighted that a proper choice of the transducers is determinant to apply successfully the proposed methodology. Wide bandwidth excitation pulses (short time signals) are suited to evaluate materials composed by thin layers. Hence, the central frequency, the power and the quality factor of the transducers must be carefully selected. With these considerations in mind, the NDE methodology presented can be utilized to any case where the wave which propagates through the sample can be considered as a longitudinal wave.

Acknowledgments

References

[1] W.D. Callister, D.G. Rethwisch, Material Science and Engineering: An introduction, ninth ed., Wiley e-Text, 2013. ISBN: 978-1-118-54689-5.

[2] K.K. Chawla, Composite Materials. Science and Engineering, third ed., Springer, New York, 2012. ISBN: 978-0-387-34365-3 (e-Book).

[3] P.K. Levangie, C.C. Norkin, Joint Structure and Function. A Comprehensive Analysis, fifth ed., F.A. Davis Company, 2011. ISBN-13: 978–0803623620.

[4] J. Dougal, N. Petford, The Field Description of Igneous Rocks, second ed., Wiley, 2011. ISBN: 978-1-119-95717-1.

[5] H. Li, J.J. Vlassak, Determining the elastic modulus and hardness of an ultrathin film on a substrate using nanoindentation, J. Mater. Res. 24 (3) (2009) 1114–1126.

[6] D. Josell, D. van Heerden, D. Shechtman, D. Read, Mechanical properties of multilayer materials, Nanostruct. Mater. 12 (1999) 405–408.

[7] P.C. Pedersen, I. Lifshitz, Ultrasound system for acoustic impedance profile reconstruction, in: IEEE Engineering in Medicine and Biological Society 10th Annual Conference, 1988.

[8] J.B.C. Leite, J.L. San Emeterio, W.C.A. Pereira, Reflection and Transmission of Plane Ultrasonic Pulses in a Three Layers Biological Structure, International Congress of Acoustics, ICA, Madrid, 2007.

[9] G. Kino, Acoustic Waves: Devices, Imaging and Analogue Signal Processing, Prentice-Hall, 1987.

[10] J.D.N. Cheeke, Non-destructive Evaluation (NDE) of Materials in Fundamentals and Applications of Ultrasonic Waves, CRC Press LLC, 2002.

[11] S.R. Singiresu, The Finite Element Method in Engineering, fourth ed., Elsevier Butterworth-Heinemann, 2005.

[12] O.P. Gupta, Finite and Boundary Element Methods in Engineering. A.A. Balkena, a member of Swets & Zeitlinger Publishers, 1999.

[13] G.D. Smith, Numerical Solution of Partial Differential Equations. Finite Difference Method, third ed., Clarendon Press, Oxford, 1985.

[14] G. Rus, J. García-Martínez, Ultrasonic tissue characterization for monitoring nanostructured TiO_2-induced bone growth, Phys. Med. Biol. 52 (2007) 3531–3547.

[15] J. Rosenbaum, Bulk Acoustic Waves Theory and Devices, Artech House Inc, Norwood, USA, 1988.

[16] S.R. Ghorayeb, E. Maione, V. La Magna, Modelling of ultrasonic wave propagation in teeth using PSpice. A comparison with finite element model, IEEE Trans. UFFC 48 (4) (2001) 1124.

[17] N. Bochud, Procesado de señal para evaluación no destructiva ultrasónica. Tesis de Maestría en Sistemas Multimedios, Univ. de Granada, 2010.

[18] A.A. Fahim, R. Gallego, N. Bochud, G. Rus, Model-based damage reconstruction in composites from ultrasound transmission, Composites Part B 45 (2013) 50–52.

[19] N. Bochud, M. Gómez Ángel, G. Rus, J.L. Carmona, A.M. Peinado, Robust parametrization for non-destructive evaluation of composites using ultrasonic signals, in: Proc of IEEE International Conference on Acoustics, Speech, and Signal Processing, Prague, 2011. pp. 1789–1792.

[20] N. Cretu, G. Nita, Pulse propagation infinite elastic inhomogeneous media, Comput. Mater. Sci. 31 (2004) 326–336.

[21] F. Hägglund, J.E. Carlson, T. Anderson, Ultrasonic classification of thin layers within multi-layered materials, Meas. Sci. Technol. 21 (2010). 015701 (9 pp).

[22] M.G. Messineo, G.L. Frontini, G.E. Eliçabe, Luis F. Gaete-Garretón, Equivalent ultrasonic impedance in a multilayer media. A parameter estimation problem, Inverse Probl. Sci. Eng. 21 (8) (2013) 1268–1287, http://dx.doi.org/10.1080/17415977.2012.757312.

[23] G. Mavko, T. Mukerji, J. Dvorkin, The Rock Physics Handbook, Cambridge University Press, 2003 (paperback) ISBN 0-521-54344-4.

[24] J. Krautkrämer, H. Krautkrämer, W. Grabendörfer, L. Niklas, Ultrasonic Testing of Materials, Springer-Verlag, Berlín, 1969.

[25] W. Chen, S. Holm, Fractional Laplacian time-space models for linear and nonlinear lossy media exhibiting arbitrary frequency power-law dependency, J. Acoust. Soc. Am. 115 (4) (2004).

[26] T.L. Szabo, Time domain wave equation for lossy media obeying a frequency power law, J. Acoust. Soc. Am. 96 (1) (1994).

[27] J.E. Dennis, R.B. Schnabel, Numerical Methods for Unconstrained Optimization and Nonlinear Equations, SIAM, 1996.

[28] S. Umchid, Frequency dependent ultrasonic attenuation coefficient measurement, in: Third International Symposium on Biomedical Engineering, 2008, pp. 234–238.

[29] M.G. Messineo, Análisis inverso de señales ultrasónicas aplicado a la caracterización de materiales en capas, Tesis doctoral, UNMDP, 2014.